CAV2021
11th International Symposium on Cavitation
May 10-13, 2021, Daejon, Korea

A Numerical Model for Nonspherical Microbubbles Using A Coupled Level Set and Volume-Of-Fluid Method

[1]Bashir M. Alnajar[1], Indrajit Chakraborty[2] and Michael L. Calvisi[1*]

[1]Department of Mechanical and Aerospace Engineering, University of Colorado Colorado Springs, USA
[2]Mathematics Institute, University of Warwick, UK

Abstract: The coupled level set and volume-of-fluid (CLSVOF) method is an efficient approach used to simulate multiphase flows in which fluids of different phases are separated by a complex, evolving interface. This method leverages the advantages of both the level set (LS) and volume-of-fluid (VOF) approaches by combining the strong mass conservation properties of the VOF method, while retaining the accurate interface representation of the LS method. In this work, the flow field is discretized by a single-field, finite difference formulation of the weakly compressible Navier-Stokes equations on a stationary grid. A coupled second-order operator split algorithm is used to advect the volume fraction and level set function, and the interface is reconstructed using the least-squares volume-of-fluid interface reconstruction algorithm (LVIRA). A numerical code has been developed for two-dimensional and axisymmetric geometries. The code performance has been validated through a series of test cases, such as the oscillation of a spherical bubble in response to changes in ambient pressure. The nonspherical dynamics of microbubbles subject to an oscillatory pressure are investigated near a rigid boundary.

Keywords: level set method, volume-of-fluid method, CLSVOF method, microbubbles, ultrasound contrast agents, nonspherical bubbles, microjet

1. Introduction

Encapsulated microbubbles (EMBs) were originally developed for diagnostic medical imaging as ultrasound contrast agents (UCAs) [1]. More recently, they are being explored for a variety of therapies that include use as drug and gene delivery vehicles [2], for opening the blood-brain barrier [3], and for tissue destruction (thrombolysis). The high compressibility of EMBs in response to ultrasound and their small size, on the order of 1-10 μm, make them applicable and safe for use in biomedical applications. Nonspherical bubble shapes, in which the radius of curvature varies along the interface, often arise due to asymmetric disturbances in the surrounding flow. These disturbances can occur, for example, when there are pressure gradients, or nearby rigid boundaries or bubbles. Most existing models of EMBs assume the bubble is spherical. However, highly nonspherical oscillations, as occur in strong bubble collapse, can only be understood through numerical methods. One of the primary challenges of numerically simulating a bubble is tracking the evolving interface between the liquid and the gas, and one method that has been developed to address this challenge is the coupled level set and volume-of-fluid (CLSVOF) method [4]. We develop a multiphase solver from the ground up, which combines the advantages of the level set (LS) and volume-of-fluid (VOF) methods. Our solver can be used to simulate incompressible or weakly compressible flow in two-dimensional and axisymmetric geometries. The capability of the solver to simulate multiphase flows with large density and viscosity ratios, on the order of 1:1000 and 1:100, respectively, is demonstrated.

2. Method

* Corresponding Author: Michael L. Calvisi, mcalvisi@uccs.edu

We follow the work of Chakraborty [5] who used a single-fluid continuum formulation in which both the gas and liquid phases are treated as a single fluid by considering the change in physical properties across the interface. In this formulation, we solve for a single continuity equation and a single momentum equation throughout the whole flow domain, considering the corresponding physical properties in each phase. One benefit achieved from this approach is a continuous velocity field that leads to continuity of the normal and tangential velocities across the interface for viscous fluids. Using the CLSVOF method, the governing equations (continuity and momentum) for the weakly compressible single-fluid formulation are

$$\nabla \cdot \mathbf{u} = -\frac{(1-F)}{\gamma p}\frac{Dp}{Dt} \tag{1}$$

$$\frac{\partial(\rho \mathbf{u})}{\partial t} + \nabla \cdot (\rho \mathbf{u}\mathbf{u}) = -\nabla p + \nabla \cdot \left[\mu(\nabla \mathbf{u} + \nabla \mathbf{u}^T) - \frac{2}{3}\mu(\nabla \cdot \mathbf{u})\mathbf{I}\right] + \boldsymbol{f_s} \tag{2}$$

$$\frac{(1-F)}{\gamma p^0}\frac{dp^0}{dt} = -\nabla \cdot \mathbf{u} \tag{3}$$

where $\mathbf{u}$ is the velocity vector, t is time, and ρ and μ are the density and viscosity of the single phase, respectively, which depend on the location relative to the interface. In addition, $\mathbf{I}$ is the identity tensor, $\boldsymbol{f_s}$ is the surface force per unit volume tensor, F is the liquid volume fraction, and γ is the polytropic exponent, which is equal to unity for isothermal motion of the gas and is equal to the ratio of specific heats for adiabatic motion. Here, p denotes a unique (single) pressure that contains both the time-varying and spatially uniform thermodynamic pressure, $p^0(t)$, and the hydrodynamic pressure, which varies spatially [5]. From continuity equations (1) and (3), the value of the liquid volume fraction determines the compressibility condition. For example, if the computational grid cell is completely filled with liquid, $F = 1$, the divergence of the velocity is zero, and the incompressibility assumption is enforced. Otherwise, if the computational grid cell is partially full of gas, $0 < F < 1$, or fully occupied by the gas, $F = 0$, the divergence of the velocity does not vanish, and the compressible assumption holds. The instantaneous spatial distribution of ρ and μ is determined by the level set function, ϕ, which evolves depending on the computed flow fields, as follows:

$$\rho = \rho_g + (\rho_l - \rho_g)H_\varepsilon(\phi) \tag{4}$$

$$\mu = \mu_g + (\mu_l - \mu_g)H_\varepsilon(\phi) \tag{5}$$

where the subscripts g and l represent the gas and liquid phases, respectively, and the smoothed Heaviside function, $H_\varepsilon(\phi)$, is defined as given in [6]. The surface tension is modeled as a body force, concentrated in a narrow band around the interface in order to reduce the lack of regularity in the solution of the governing equations that results from singular source terms. Here, $\boldsymbol{f_s} = \sigma\kappa(\phi)\mathbf{n}(\phi)\delta_\epsilon(\phi)$, as reported by Chang et al. [7], where σ is the surface tension coefficient assumed to be constant, and $\kappa(\phi)$ and $\mathbf{n}(\phi)$ are the local interface curvature and unit normal vector, respectively. The delta function $\delta_\varepsilon(\phi)$ is defined as the derivative of the one-dimensional Heaviside function as $\delta_\varepsilon(\phi) = H'_\epsilon(\phi)$. For further details about the numerical method and computational domain used, refer to Alnajar [8].

3. Results

In this section, we validate our axisymmetric, weakly compressible CLSVOF solver in modeling essential features of bubble dynamics.

* Corresponding Author: Michael L. Calvisi, mcalvisi@uccs.edu

3.1. Spherical Oscillation of a Gas Bubble

First, we evaluate the accuracy of our axisymmetric weakly compressible CLSVOF code by performing several simulations of oscillating free gas bubbles and comparing the radius vs. time curves with numerical solutions of the Rayleigh-Plesset equation (RPE) [9]. The simulations start with a spherical bubble centered at the midpoint of the line of axisymmetry (z-axis). The effect of gravity is neglected. The gas bubble oscillates due to a change in the far-field pressure, p_∞, for $t > 0$, which is imposed on the computational domain boundaries and can be constant or variable, according to

$$p_\infty = \begin{cases} p_{atm} & \text{if} \quad t \le 0 \\ \text{Constant: } p_{atm}(1 + p_{ac}) & \text{if} \quad t > 0 \\ \text{Variable: } p_{atm}\left(1 + p_{ac} sin\left(2\pi f_p t\right)\right) & \text{if} \quad t > 0 \end{cases}$$

where $t \in [0, T]$ is the simulation time, p_{atm} is a constant hydrostatic pressure, p_{ac} is a dimensionless driving pressure, and f_p is the acoustic frequency. Simulations were carried out for a bubble with initial radius $R_0 = 50$ μm, which was subjected to constant and variable pressures, as indicated in Eq. (7), using two relatively coarse mesh densities of 100 × 100 and 200 × 200. To minimize numerical errors due to the proximity of the far-field pressure imposed as boundary conditions, the domain boundaries are placed sufficiently far from the bubble interface and are located a distance $16R_0$ from the origin. Figure 1 compares the radius vs. time curves of the CLSVOF model (dashed lines) to the solution of the RPE (solid lines) and shows that our solver can match the predictions of the RPE with good accuracy. We note that the simulation results converge to the RPE solution as the mesh density increases; however, there is a noticeable discrepancy, especially as the number of oscillations increases.

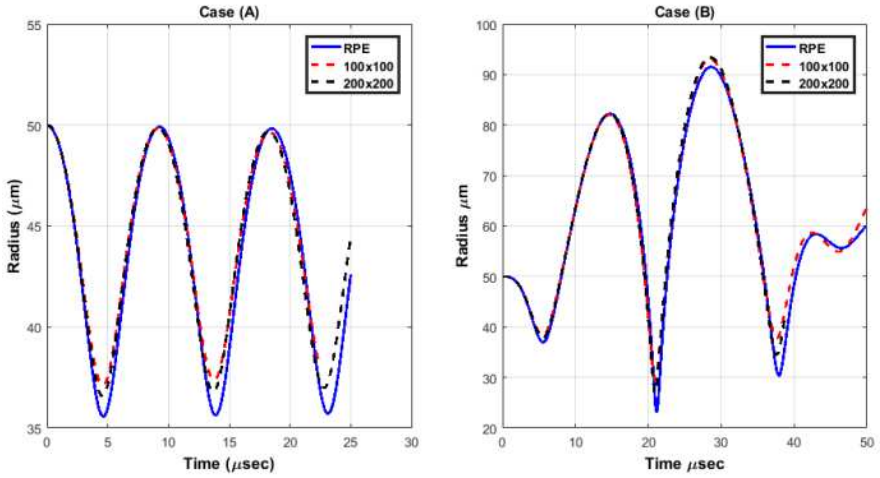

Figure 1. Comparison of the bubble radius vs. time obtained from the weakly compressible CLSVOF solver (dashed lines) and the Rayleigh-Plesset equation (solid line) with $R_0 = 50$ μm. Case (A): constant pressure. Case (B): variable pressure with $f_p = 80$ kHz. The liquid and gas parameters are: $p_{atm} = 10^5$ Pa, $p_{ac} = 10^0$, $\rho_l = 1000$ kg/m^3, $\rho_{g,0} = 1$ kg/m^3, $\mu_l = 0.001$ Pa-s, $\mu_g = 10^{-5}$ Pa-s , $\sigma = 0.0720$ N/m, and $\gamma = 1.4$, where $\rho_{g,0}$ is the initial gas density. The number of grid points used was 100 × 100 and 200 × 200.

3.2. Nonspherical Bubble Collapse Near a Rigid Boundary

In this section, we numerically simulate an initially spherical bubble collapsing near a rigid boundary by applying a no-slip boundary condition to the bottom edge of the domain. We consider an air bubble with initial radius, $R_0 = 180$ μm, surrounded by water. The liquid and gas properties used are the same as

* Corresponding Author: Michael L. Calvisi, mcalvisi@uccs.edu

those shown in the Figure 1 caption except that $\sigma = 0.0434$ N/m and $\gamma = 1.304$. The bubble is initially at rest in a square domain with dimensions $13R_0 \times 13R_0$ and its center is located at a standoff distance $h_0 = 1.5R_0$ from a rigid wall, which is coincident with the bottom edge of the domain. We impose a sinusoidally-varying far-field pressure, p_∞, per Eq. (7) with $p_{ac} = 10^0$ and $f_p = 4.17$ kHz along the side and top edges of the domain. The number of grid points used is 100×100. In Figure 2 is shown the nonspherical shape evolution of the air bubble near a rigid surface. The initially spherical bubble grows rapidly until it reaches its maximum size at $t \approx 0.2268$ ms. Then, the bubble starts shrinking and collapses. During the later stages of collapse, a high-speed jet develops on the distal side of the bubble and penetrates through the bubble in a direction perpendicular to the boundary. The jet pierces the opposite bubble wall at $t \approx 0.2664$ ms and subsequently transforms the bubble shape into a torus. Figure 2 also shows the pressure and the velocity vectors in the flow field during the growth and collapse stages. The pressure within the bubble decreases as the bubble expands. During collapse, the far-field pressure increases and the surrounding liquid reverses direction and compresses the bubble, causing it to contract rapidly, decrease in volume, and further deform nonspherically. A large pressure difference develops across the top and bottom surfaces of the bubble, which is on the order of 1.2 MPa, and a high-speed jet is generated with velocity $v_{jet} = 246$ m/s on the upper wall of the bubble at $t \approx 0.264$ ms.

The results of Figure 2 compare qualitatively well with prior experimental and numerical results of bubbles collapsing near a rigid surface, including the recent experimental measurements by Reuter and Kaiser [10]. In an additional simulation not shown here, a gas bubble driven by an acoustic standing wave near a rigid boundary with standoff distance $h_0 = 2.0R_0$ was simulated and compared against the results of Sato et al. [11] who used the boundary integral method to simulate the same case. The results of the present CLSVOF solver compare very closely with those of Sato et al., both quantitatively and qualitatively, in terms of the shape evolution of the bubble, volume, and period of collapse.

4. Conclusions

In this work, we presented a multiphase flow solver based on the CLSVOF method of Chakraborty [5] and validated its effectiveness by conducting simulations of a spherical gas bubble in an infinite liquid and of a nonspherical bubble driven by an oscillatory pressure near a rigid boundary.

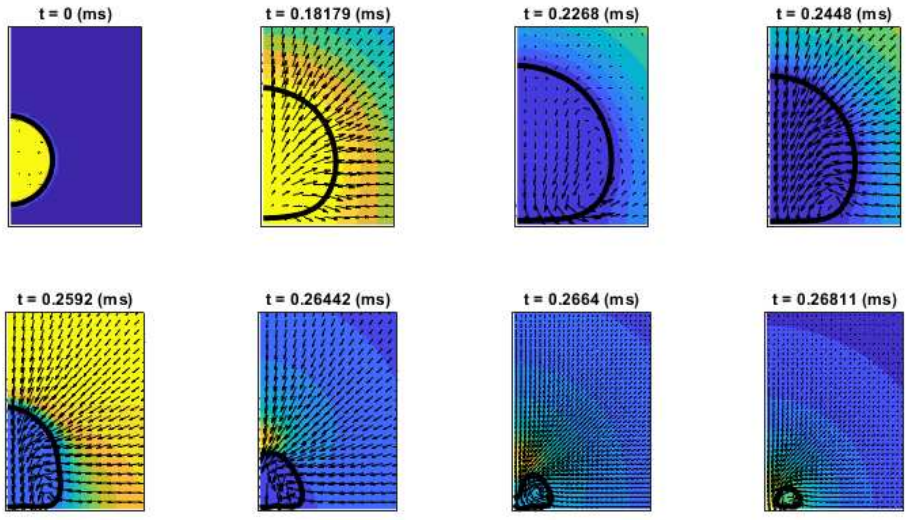

Figure 2. Simulation of a nonspherical air bubble with $h_0 = 1.5R_0$ showing the shape evolution, velocity vectors, and pressure contours in the near-wall region during growth, collapse, and jet impact. A rigid boundary is located along the bottom edge. Blue indicates low pressure and yellow indicates high pressure.

* Corresponding Author: Michael L. Calvisi, mcalvisi@uccs.edu

Acknowledgments: We acknowledge NSF CAREER Award 1653992 and the College of Engineering and Applied Science at the University of Colorado Colorado Springs for providing funding support.

References

1. Ferrara, K.; Pollard, R.; Borden, M. Ultrasound microbubble contrast agents: Fundamentals and application to gene and drug delivery. *Annual Review of Biomedical Engineering* **2007**, *9*, pp. 415-447.
2. Fan, Z.; Kumon, R.E.; Deng, C.X. Mechanisms of microbubble-facilitated sonoporation for drug and gene delivery. *Therapeutic Delivery* **2014**, *5*, pp. 467-486.
3. Lee, H.; Kim, H.; Han, H.; Lee, M.; Lee, S.; Yoo, H.; Chang, J.H.; Kim, H. Microbubbles used for contrast enhanced ultrasound and theragnosis: A review of principles to applications. *Biomedical Engineering Letters* **2017**, *7*, pp. 59-69.
4. Sussman, M. A second order coupled level set and volume-of-fluid method for computing growth and collapse of vapor bubbles. *Journal of Computational Physics* **2003**, *187*, pp. 110-136.
5. Chakraborty, I. Numerical modeling of the dynamics of bubble oscillations subjected to fast variations in the ambient pressure with a coupled level set and volume of fluid method. *Physical Review E* **2019**, *99*, p. 043107.
6. Sussman, M.; Puckett, E.G. A coupled level set and volume-of-fluid method for computing 3D and axisymmetric incompressible two-phase flows. *Journal of Computational Physics* **2000**, *162*, pp. 301-337.
7. Chang, Y.; Hou, T.; Merriman, B.; Osher, S. A level set formulation of Eulerian interface capturing methods for incompressible fluid flows. *Journal of Computational Physics* **1996**, *124*, pp. 449-464.
8. Alnajar, B.M. Numerical and Constitutive Modeling of Encapsulated Microbubbles: Nonspherical Deformation and Transient Network Theory. Ph.D., University of Colorado Colorado Springs, Colorado Springs, Colorado, USA, December 19, 2020.
9. Plesset, M.S.; Prosperetti, A. Bubble dynamics and cavitation. *Annual Review of Fluid Mechanics* **1977**, *9*, pp. 145-185.
10. Reuter, F.; Kaiser, S.A. High-speed film-thickness measurements between a collapsing cavitation bubble and a solid surface with total internal reflection shadowmetry. *Physics of Fluids* **2019**, *31*, p. 097108.
11. Sato, K.; Tomita, Y.; Shima, A. Numerical analysis of a gas bubble near a rigid boundary in an oscillatory pressure field. *Journal of the Acoustical Society of America* **1994**, *95*, pp. 2416-2424.

* Corresponding Author: Michael L. Calvisi, mcalvisi@uccs.edu